Meteorological and hydrological data from the Alder Creek watershed, SW Ontario

Andrew J. Wiebe[1,2], David L. Rudolph[1]

[1]Department of Earth and Environmental Sciences, University of Waterloo, Waterloo, N2L 3G1, Canada
5   [2]Department of Earth and Planetary Sciences, McGill University, Montreal, H3A 0E8, Canada

Correspondence to: Andrew J. Wiebe (ajwiebe@uwaterloo.ca)

Abstract. Data for small to mid-sized watersheds are seldom publicly available but may be representative of diverse types of hydrological contexts when assessing patterns. These types of data may also prove valuable for informing numerical experimentation and practical modelling. This paper presents data collected in the Alder Creek watershed, located within the

10   Grand River basin in Ontario, Canada. The Alder Creek watershed provides source water from the aquifers of the Waterloo Moraine for multiple well fields that supply the cities of Kitchener and Waterloo. Recharge rates and human impacts on streamflow are important topics for the watershed, and many numerical models of the area have been constructed. In order to support these types of analyses, field equipment was deployed within the watershed between 2013 and 2018 to monitor groundwater levels, stream stage, soil moisture, soil temperature, rainfall, and other weather parameters. The available data

15   are described, complementary information is presented, and examples of possible analyses are cited and illustrated. The data presented and described in this paper are available at https://doi.org/10.20383/101.0178 (Wiebe et al., 2019).

1 Introduction

Comprehensive meteorological and hydrological data from multiple field stations within small to mid-sized watersheds are seldom publicly available. This lack of data hinders the comparison of watersheds in different areas and the analysis of

20   hydrological patterns across the entire spectrum of watershed sizes. For instance, the spatial correlation structure of rainfall within a particular type of region may be poorly represented in the literature and therefore unavailable to verify or enhance regional models.

Moraines in southern Ontario are frequently used for public drinking water supply. Groundwater wells draw water for public supply from unconsolidated aquifers, which are replenished by (e.g., Lerner, et al., 1990; Wiebe, 2020): 1) rain

25   and snowmelt percolation through the vadose zone that arrives at the water table (diffuse recharge), 2) localized or depression focused recharge (DFR) that may occur in hummocky terrain, and 3) losing stream reaches (indirect recharge). This recharge is spatially variable and may vary in terms of its quality based on sources of contamination at the ground surface. The vulnerability of public supply wells to contamination is often assessed using numerical models, which require data ranging from groundwater levels to streamflow rates to precipitation amounts and evapotranspiration estimates.

30   Groundwater recharge is a generally a calculated flux that occurs in the subsurface and is a major factor influencing simulated water levels; it is very difficult to measure directly and to quantify over large, heterogeneous areas.

    The Alder Creek watershed is a typical southern Ontario watershed and has been the subject of numerous studies (e.g., CH2MHILL and SSPA, 2003; Matrix and SSPA, 2014; Sousa et al., 2013; Wiebe and Rudolph, 2020) due to its importance for local water supply. The Southern Ontario Water Consortium (SOWC; now called the Ontario Water

35   Consortium, www.ontariowater.ca) undertook to instrument the Alder Creek watershed as part of a project to set up a platform for testing new sensor technologies and to collect hydrological data. Research questions related to the installed equipment included topics such as how sensitive modelled groundwater recharge estimates might be to spatially variable rainfall (Wiebe and Rudolph, 2020), how recharge dynamics respond to extreme hydrological events (Menkveld, 2019), and how depression focused recharge might increase threats to public supply wells (Wiebe, 2020; Wiebe et al., 2021). The Alder

40   Creek watershed was the middle member of a continuum of three watersheds along a spectrum of urbanization that varied from fully urbanized (Mimico Creek, Greater Toronto Area, ON; 77 km^2; TRCA, 2018) to rural/agricultural (Hopewell Creek, east of Kitchener, ON; 72 km^2; Irvine, 2018). Hydrological equipment was installed in the Alder Creek watershed between 2013 and 2019. The following summarizes the datasets that have been made available on the Federated Research Data Repository (www.frdr-dfdr.ca/repo/), shows example graphs, and presents complementary information including

45   borehole logs, piezometer construction descriptions, and analyses related to the dataset.

2 Site description

The Alder Creek watershed (Fig. 1; 78 km^2; e.g., described by Wiebe, 2020) is located on the Waterloo Moraine southwest of the cities of Waterloo and Kitchener in southern Ontario, Canada (43.3982° N, 80.5455° W). The Waterloo Moraine consists of alternating coarse and fine layers of unconsolidated sediments (Martin and Frind, 1998) deposited at the

50   confluence of multiple glacial ice lobe advances during the most recent deglaciation (Bajc et al., 2014). Alder Creek (a 4th order Strahler stream; OMNRF, 2015) is a tributary of the Nith River, which flows into the Grand River (basin area: 6,900 km^2). The quaternary geology of the watershed consists of sand and gravel units that are present over half of the watershed area, and less permeable units such as silt and clay glacial tills (OGS, 2010). Agriculture is the predominant land use (70 %) in the watershed (OMNR, 2008; ROW, 2010). The Alder Creek watershed is an important source of recharge and supplies

55   source water for up to seven public well fields (Brouwers, 2007).

    Figure 1 shows long−term and short−term monitoring locations near the watershed. A Water Survey of Canada (WSC) stream gauging station near New Dundee (02GA030; WSC, 2019) is located within the watershed on the main branch of Alder Creek, and an Environment Canada weather station at Roseville (Government of Canada, 2019) reports temperature and precipitation < 3 km outside the watershed. The University of Waterloo weather station

60   (weather.uwaterloo.ca; Seglenieks, 2020) also reports weather data in the area. Figure 2 provides the general context of major water budget components and shows that average monthly precipitation (Government of Canada, 2019) varies by up

to 40 mm at the Roseville station and that the precipitation and potential evapotranspiration (PET) peaks occur in the same season, mid–summer (Wiebe, 2020). Streamflow peaks in late winter around March.
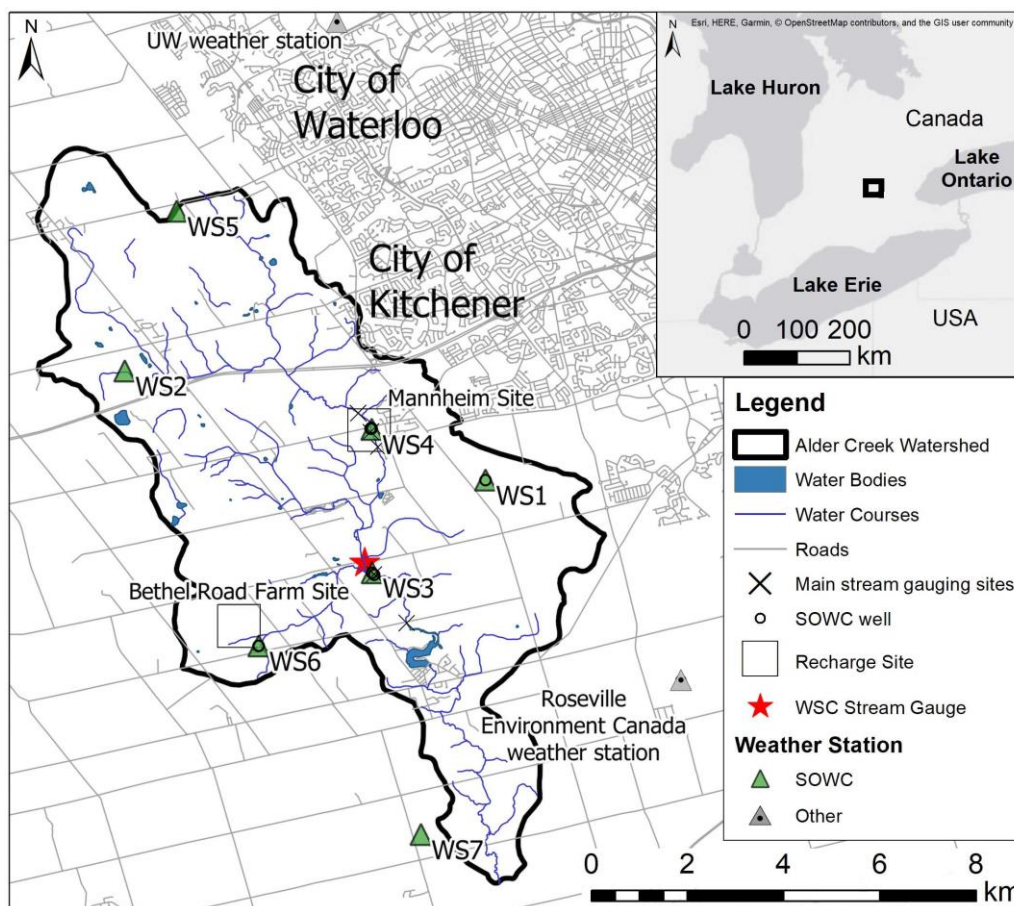
65

Figure 1: Map of Alder Creek watershed and data collection locations (Esri et al., 2020b [Sources: Esri, HERE, Garmin, © OpenStreetMap contributors, and the GIS User Community]; DMTI, 2011; Government of Canada, 2019; GRCA, 1998, Seglenieks, 2020; Wiebe et al., 2019).
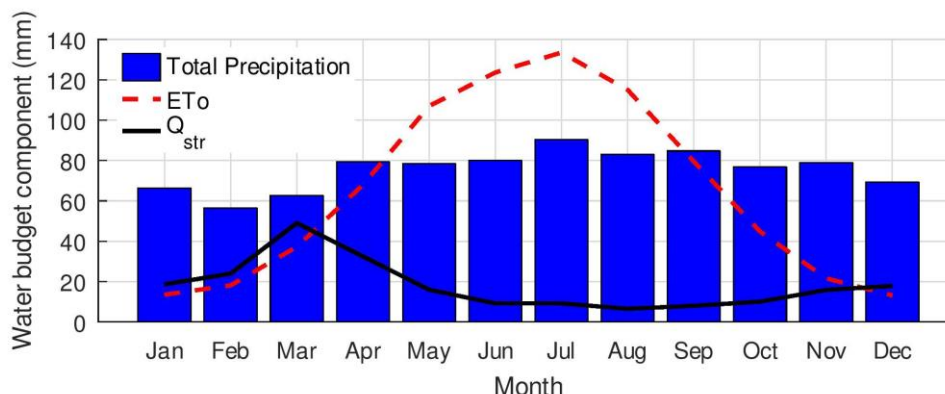
Figure 2: Major water budget component estimates for the Alder Creek watershed (adapted from Wiebe, 2020; based on data from: Government of Canada, 2019; WSC, 2019; and Wiebe et al., 2019). Reference ET (ETo) estimates were calculated via the Penman−Monteith method (Raes, 2009). Streamflow (Q_{str}) was estimated for the watershed outlet based on a scaling factor.

Equipment installations during the SOWC – Alder Creek project included weather stations, recharge stations, and stream stations (Fig. 1). Seven weather stations were installed in and around the watershed. Two sites (the Mannheim site and the Bethel Road Farm site; Fig. 1) were instrumented to monitor vadose zone drainage and groundwater levels, and to estimate recharge rates. These recharge sites are shown in more detail in Fig 3. Twenty observation wells (including three drive−point streambed piezometers) were installed at the Mannheim site, and 15 observation wells were installed at the Bethel Road Farm site. Soil moisture and subsurface temperature were monitored at these two sites. Five locations along the creek were instrumented with pressure transducers to monitor surface water levels and temperatures. Stream gauging and the development of rating curves at these locations was conducted to augment the records at the WSC gauge within the watershed.
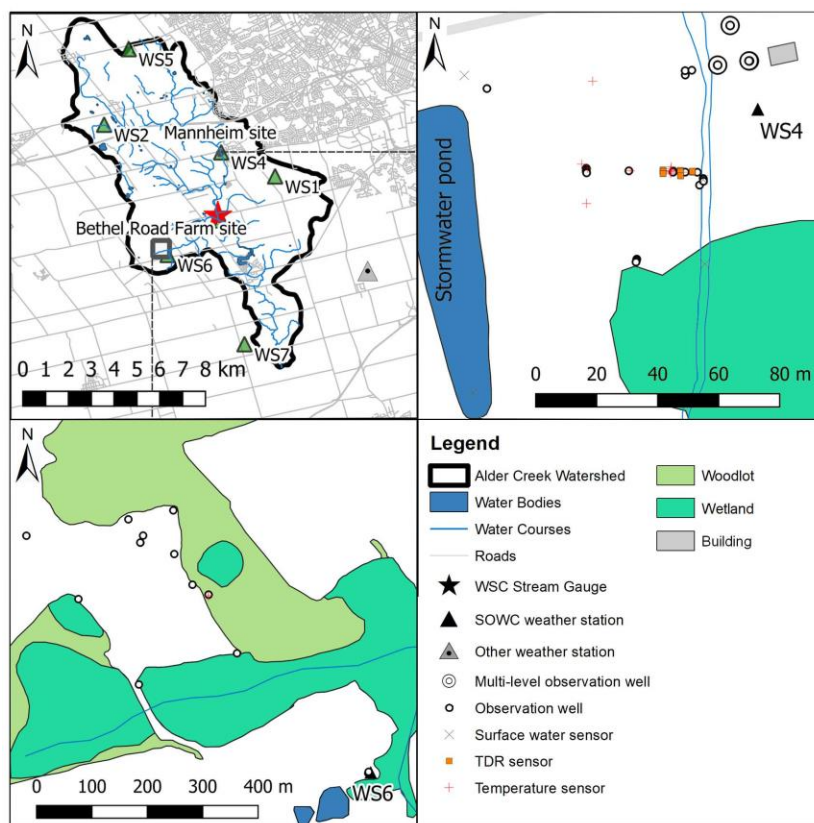
Figure 3: The Mannheim and Bethel Road Farm "Recharge" sites (woodlots, wetlands, and buildings adapted from Esri et al., 2020a [Sources: Esri, HERE, Garmin, Intermap, INCREMENT P, GEBCO, USGS, FAO, NPS, NRCAN, GeoBase, IGN, Kadaster NL, Ordnance Survey, Esri Japan, METI, Esri China (Hong Kong), © OpenStreetMap contributors, GIS User Community]; DMTI, 2011; Government of Canada, 2019; GRCA, 1998; Wiebe et al., 2019).

3 Meteorological data

Seven weather stations (Fig. 1; WS1 to WS7) were installed during the SOWC – Alder Creek project to monitor spatially variable precipitation and parameters related to evapotranspiration in the area. Figure 4 shows photos of two weather stations as examples, and the components of the stations are listed in Table 1. Data were typically downloaded hourly from the stations to a computer at the University of Waterloo (Waterloo, Ontario, Canada) via the cellular telephone network.

Figure 4: Photos of weather stations: a) WS2 (shown prior to installation of windscreen around rain gauge), and b) WS4.

Data from the weather stations was reviewed and missing time stamps were assigned placeholders (e.g., "#N/A") to
100   indicate "not available." Anomalous data values, i.e., values outside of an acceptable range for the parameter and the season,
were similarly assigned placeholders. Despite this, occasional erroneous values and error codes may still be present, and the
data should be reviewed for quality prior to use.

Figure 5 presents example weather data and derived (Penman−Monteith) PET (Raes, 2009) estimates at WS2.
Similar records are available for each of the seven stations, although there are systemic differences depending on where the
105   stations were located within the watershed. Average air temperature (e.g., Fig. 5a) derived from 15 min time intervals ranged
from -34.7 °C to +32.9 °C between Jan 2014 and Dec 2018, based on data from all seven stations. Consistent differences
between temperatures at the seven weather stations could be related to the positioning of each sensor relative to local
vegetation. Relative humidity (e.g., Fig. 5b) ranged from 16 to 100 % across all stations. Wind speeds (Fig. 5c) at the seven
weather stations varied from 0 m·s^{-1} to a maximum of 14.6 m·s^{-1} (WS3), with an overall average of 1.6 m·s^{-1}. Knowledge of
110   the average wind speed was helpful during calculations of PET (Wiebe, 2020) when specifying a value to fill−in for missing
information. Solar radiation (Fig. 5d) was typically measured as incoming solar radiation with solar pyranometer devices and
ranged up to 1,190 W·m^{-2} at the seven weather stations. Net incoming radiation estimates at WS7 were up to 893 W·m^{-2}.
Figure 5e shows an example of the daily Penman−Monteith PET estimates derived from the WS2 data using the ETo
Calculator program (ETo: reference evapotranspiration; Raes, 2009).

115 **Table 1: Meteorological variables and instruments in the SOWC−Alder Creek network.**

Station	WS1	WS2/WS3/WS4/WS5	WS6	WS7
Record[*]	Jan 2014 – Dec 2016			
Air temperature (°C) and relative humidity (%)	HC2-S3	HMP155	HMP45C / HMP155[§]	HMP45C
Wind speed (m·s^{-1}) and wind direction (° from North) [Measurement height above ground]	R.M. Young 05103 [3 m]	R.M. Young 05103 [3 m]	R.M. Young 05103 [3 m]	R.M. Young 05103 [3 m]
Rainfall (rain gauge) [Measurement height above ground]	TE525WS / TB3[†] [1 m]	TB3 [1 m]	TB3[‖] (×2) [1 m]	TE525WS / TB3[‖] [1 m]
Snowfall (sonic snow depth)	SR50A (Nov 2014 to Apr 2015 only)	SR50A (Nov 2014 to Apr 2015 only)	SR50A (Nov 2014 to Apr 2015 only)	SR50A (Nov 2014 to Apr 2015 only)
Incoming solar radiation (W·m^{-2})	SPLite2	EQ08-SE	SPLite2/ EQ08-SE[§]	CNR1[¶]
Barometric pressure	N/A[‡]	CS106 (WS4 only)	N/A	Young 61205V
Datalogger	CR1000	Sutron 9210B	CR1000/ Sutron 9210B[§]	CR23X / CR1000
Additional instruments	Observation well: water level and temperature – PT12	N/A	Observation wells: water levels and temperatures – PT12	Soil moisture – CS616
Telemetry	RAVEN X-HSPA cellular modem	BT6801 cellular modem	BT6801 cellular modem	BT6801 cellular modem

[*] Highest quality period of record

[†] Rain gauge switched to the latter on 6 May 2014

[‡] N/A – not applicable

[§] Datalogger switched to the latter instrument on 5 Jun 2014

120 [‖] Rain gauge switched to the latter on 11 Jul 2016

[¶] WS7 used a Campbell Scientific CNR1 Net Radiometer to measure incoming and outgoing short wave and long wave solar radiation (via pyranometer and pyrgeometer)
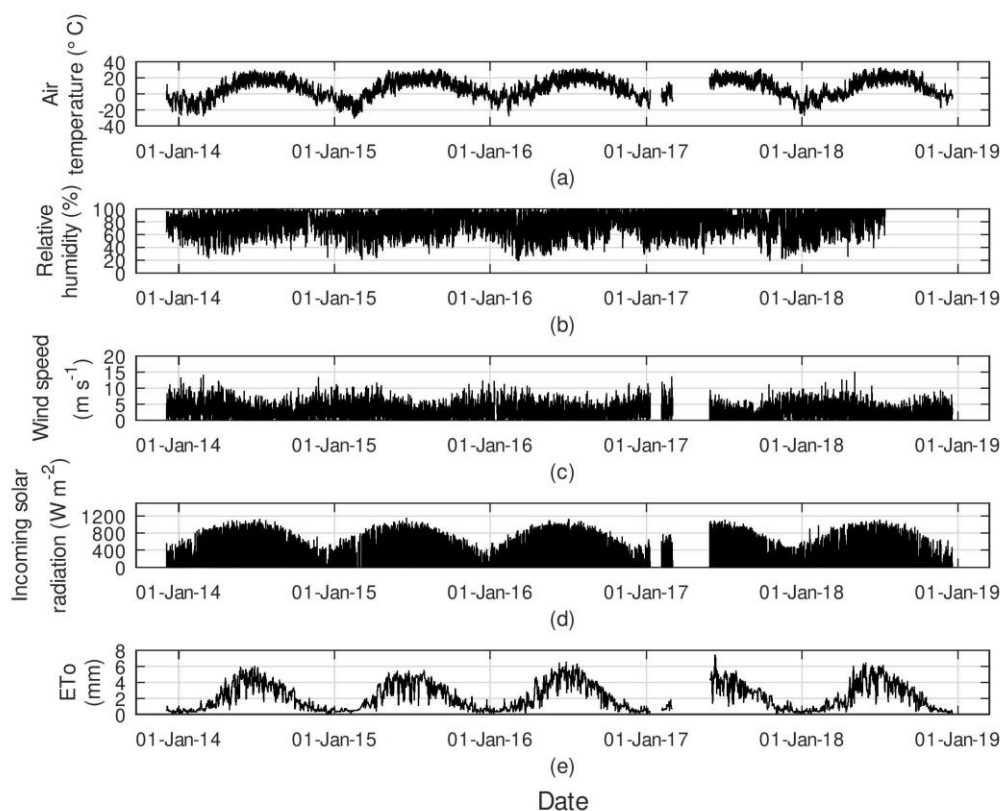
Figure 5: WS2 data (Wiebe et al., 2019) and derived Penman−Monteith PET (Raes, 2009) estimates: (a) air temperature, (b) relative humidity, (c) wind speed, (d) solar radiation, and (e) reference evapotranspiration.

Rainfall (e.g., Fig. 6) was monitored at each of the weather stations using a tipping bucket rain gauge (either Texas Instruments TE525 or Hydrological Services TB3). Each gauge was installed at a height of 1 m above ground surface and surrounded with a 1 m radius, Alter−type wind screen. A second gauge was additionally installed at station WS6 with two concentric wind screens at radii of 1 m and 2 m. Faulty wiring prevented reasonable rainfall data from being recorded at station WS1. Spatial correlation quantified via Spearman Rank Correlation coefficients among the six other weather stations and the Roseville Environment Canada weather station was between 0.5 and 0.8 (Wiebe, 2020).
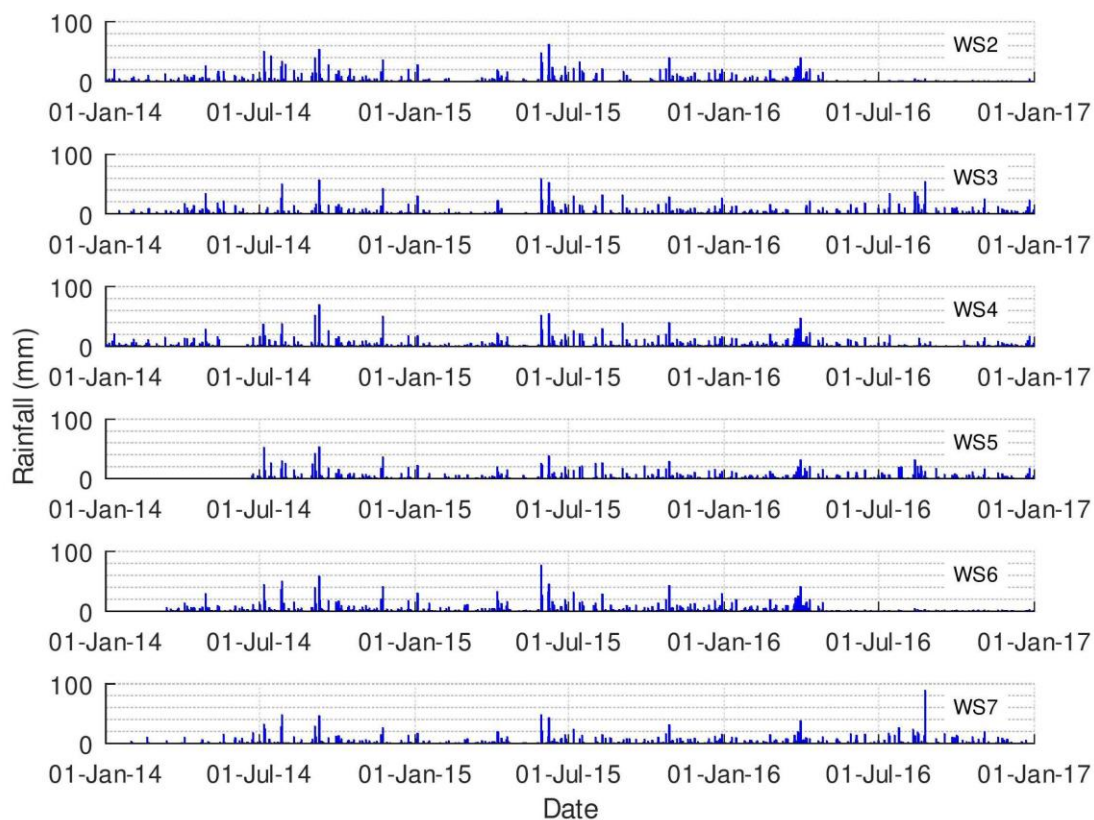
Figure 6: Daily rainfall at stations WS2 to WS7 (Wiebe et al., 2019).

135

Snowfall was monitored via sonic sensors that estimated snow depth above ground surface. The sonic snow sensors at stations WS2 to WS7 reported data for the 2014 to 2015 winter season. The snow depth data collected agree well with observations at the Roseville Environment Canada station (Fig. 7). The average from these six stations was within 2 cm of the Roseville amount on an event–by–event basis (Wiebe, 2020). Due to maintenance issues, the sonic snow sensors were only deployed for the one winter season.

140
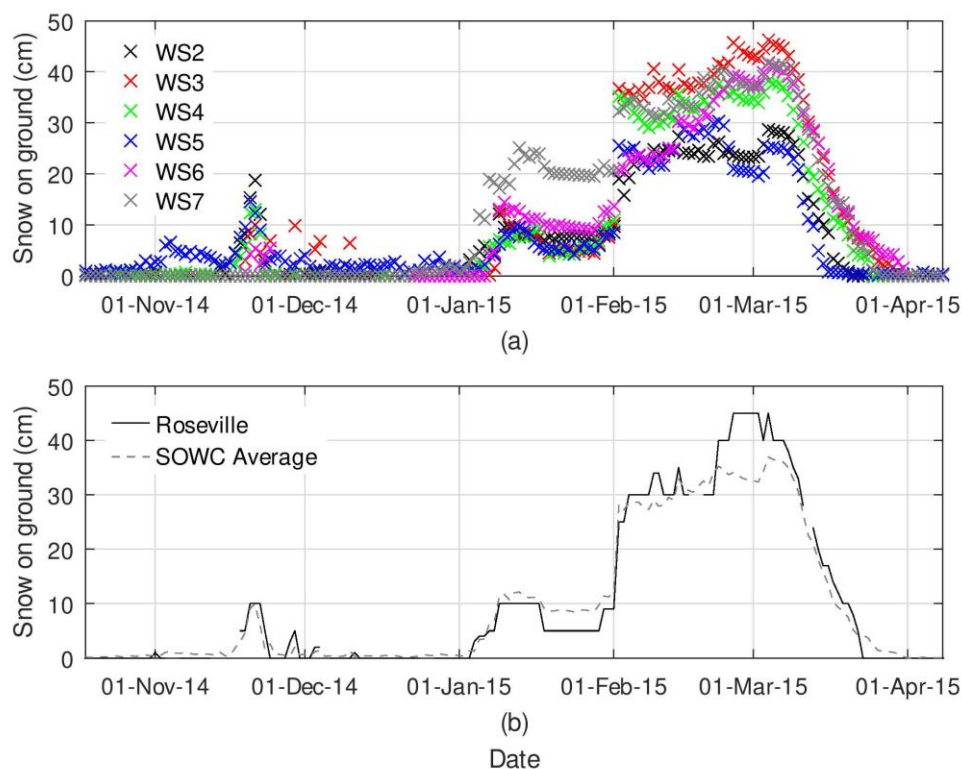
145 **Figure 7: Snowpack thickness data (a) for individual SOWC stations WS2 – WS7 (Wiebe et al., 2019), and (b) for the average from the SOWC stations and for Roseville (Government of Canada, 2019) for the 2014 to 2015 winter season (adapted from Wiebe, 2020).**

4 Groundwater data

150   Multi–level or single–screen observation wells were installed at several locations within the watershed. Borehole logs are

discussed in the next section. Pressure transducers – either vented (AquiStar PT12) or non–vented (Solinst Levelogger) –

were installed in most of the observation wells. The multi–level Solinst "Continuous Multichannel Tubing" (CMT) wells did

not have pressure transducers. Manual water level measurements were made occasionally at the wells to track water levels in

the wells without pressure transducers, or to provide adjustment targets for the pressure transducer data. Figure 8 shows an

155   example of PT12 (AquiStar Inc.) pressure transducer data from CPP3 at the Mannheim site that were adjusted based on the

average offset from manually measured water level elevations, where the sensor measurement point was originally assumed

equivalent to the bottom elevation of the piezometer screen. Solinst Levelogger data would require the additional

intermediate step of barometric pressure compensation (Solinst, 2020). Water levels fluctuated over an amplitude range

160 (maximum minus minimum water level) of up to 1.2 m over an annual cycle at background locations at the Mannheim site, i.e., locations not expected to be affected by DFR or indirect recharge beneath the stream (Wiebe, 2020). Water levels at observation wells affected by DFR (e.g., CPP2) fluctuated over a range of up to 2.4 m (Wiebe, 2020).
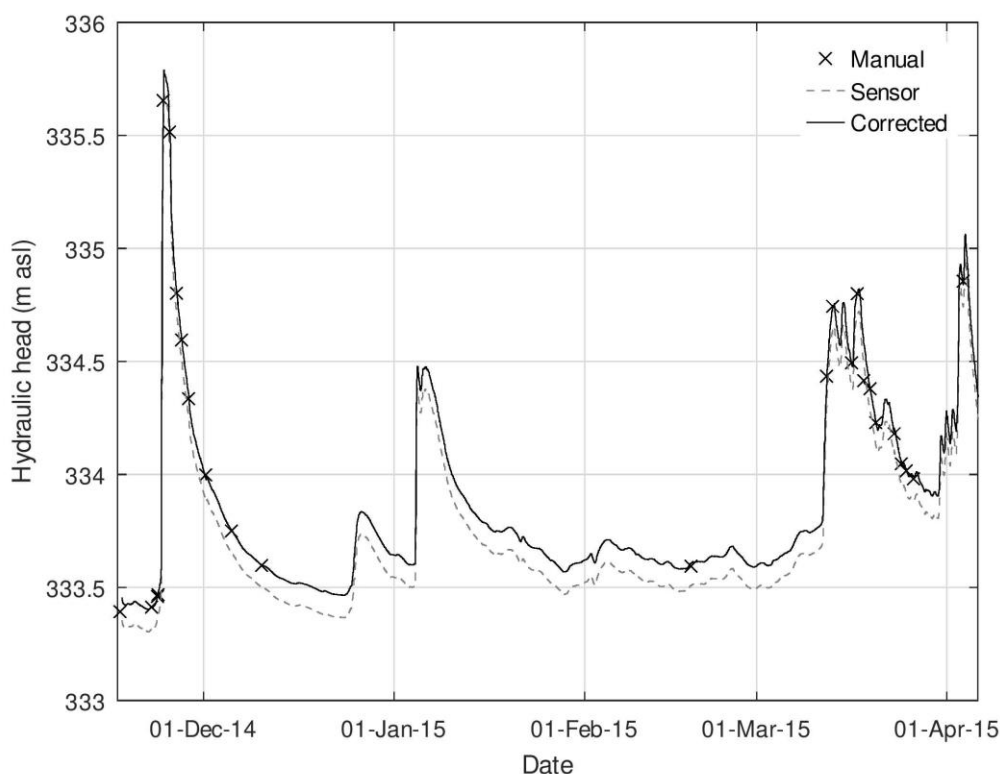
Figure 8: Adjustment of CPP3 (Mannheim site) pressure transducer data based on manual levels (Wiebe et al., 2019), with spikes
165 **due to sampling removed. Note: "m asl" indicates** *metres above sea level*.

Temperature data were recorded coincident with water levels at most of the larger–diameter wells. Figure 9 shows a selection of groundwater temperature (RTD Pt100 sensors; Metalogic Technologies, Ltd.) profiles consisting of two depths within one of the CMT wells and creek temperatures. The profiles give the approximate outline of the vertical temperature
170 envelope, which may be used to assess whether a stream reach is gaining or losing groundwater (Constantz, 2008). Alder Creek appears to be a losing stream reach during at least part of the year at the Huron Road Farm site and at the Mannheim site, based on the manual CMT water level data. Readings in the streambed drive–point piezometers at the Mannheim site occasionally indicated the presence of unsaturated soil between surface water and the water table (i.e., a water tape reading could not be made because the observation well was dry).

175
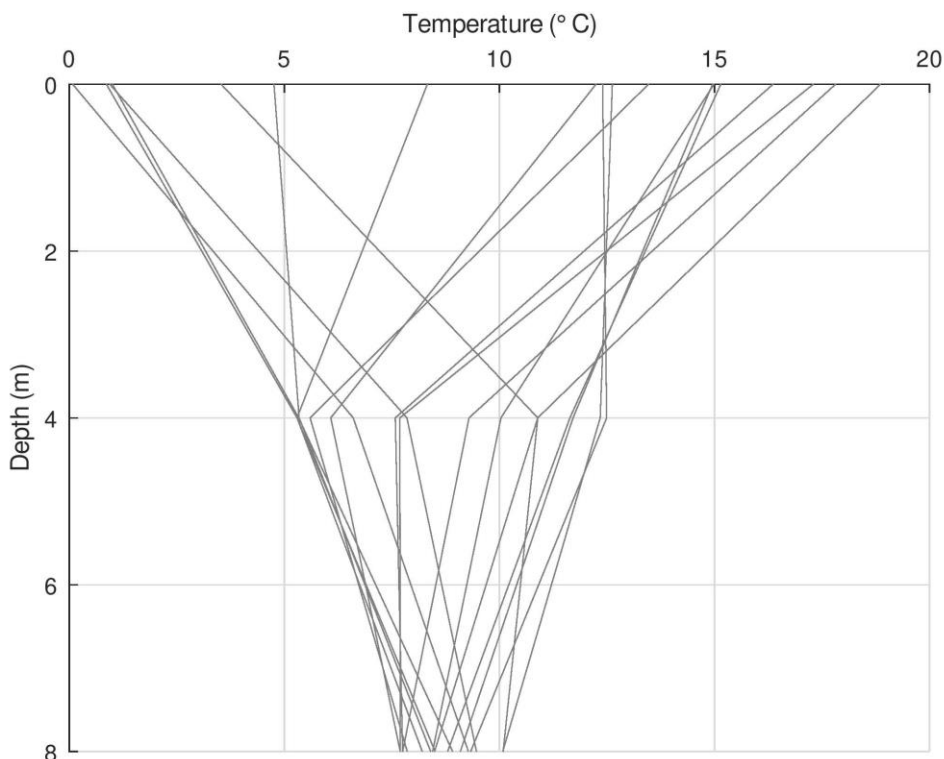
Figure 9: Daily creek (shown at 0 m depth) and adjacent CMT4 groundwater temperatures at the Huron Road Farm site (Wiebe et al., 2019). Average values from the 15th day of each month from Mar 2014 to Sep 2015 (except Dec 2014) are shown. Qualitatively, a wider annual envelope of temperature profiles suggests a losing stream reach, while a narrower envelope suggests
180 **groundwater discharge into the stream reach.**

5 Vadose zone data

Sediment samples were collected, and borehole logs were drawn for some locations. A limited number of grain size analyses were also conducted. Soil moisture and soil temperature data were collected at the two Recharge sites within the Alder Creek
185 watershed. Two different temperature methods were employed to illustrate how the data may be used to estimate vadose zone drainage rates at the Mannheim site, as discussed below.

5.1 Soil texture

The availability of borehole logs is summarized in Table 2. Borehole logs for the observation wells installed in the Alder Creek watershed were not included with the dataset, but ten logs are included below and several are available elsewhere, as

190 indicated in Table 2. Figure 10 shows the logs for three deeper wells that are described in Table 3, and Fig. 11 shows seven
shallower logs from the Bethel Road site that are described in Table 4. Grain size analyses were conducted for soil samples
from cores at three locations. Figure 12 shows results from selected coarser depth intervals at one location at the Mannheim
site and at two locations at the Bethel Road Farm site. The borehole log for MLT1 (Wiebe, 2020) at the Mannheim site
suggests silt or silty sand present in most of the borehole, with two coarser, sandy sections around depths of 0.4 m and 3.1 m.

195 The grain size analyses for this borehole support the interpretation of poorly graded, gravelly sand present around a depth of
0.4 m, and the interpretation of silty sand throughout other sections. The grain size curves for Bethel Road Farm MLT1
correspond to the associated borehole log (see Fig. 11), with finer material (sandy silt) in the uppermost sample, gravelly
sand at intermediate depths, then a more homogeneous medium sand. The grain size curves for the core adjacent to P3 at
Bethel Road Farm mostly represent fine to medium sand and generally correspond to the borehole log (Fig. 11). The gravelly

200 sand layer from 3.05 m to 4.60 m depth is well represented by the curve for 3.30 m to 3.40 m, though the subsequent lower
interval represents a more homogeneous fine sand lens or unit present within the layer.

Table 2: Overview of borehole logs.

Site / weather station	Observation well/instrument name (Provincial well tag #)	Reference
Mannheim	CMT1, CMT2a, CMT2b, CMT3	Hillier (2014)
Mannheim	Boreholes near CPP1, CPP2, CPP6, and CPP8; and at MLT1	Menkveld (2019); Appendix G in Wiebe (2020)
Bethel Road	M1, MLT1, P3, P5, P6, P7, P13	This article
WS1	(A151035)	Province of Ontario (2021), this article
WS3	CMT4 (A155063), CMT5 (A155050)	Province of Ontario (2021), this article
WS6	(A155083), (A155084)	Province of Ontario (2021), this article

205
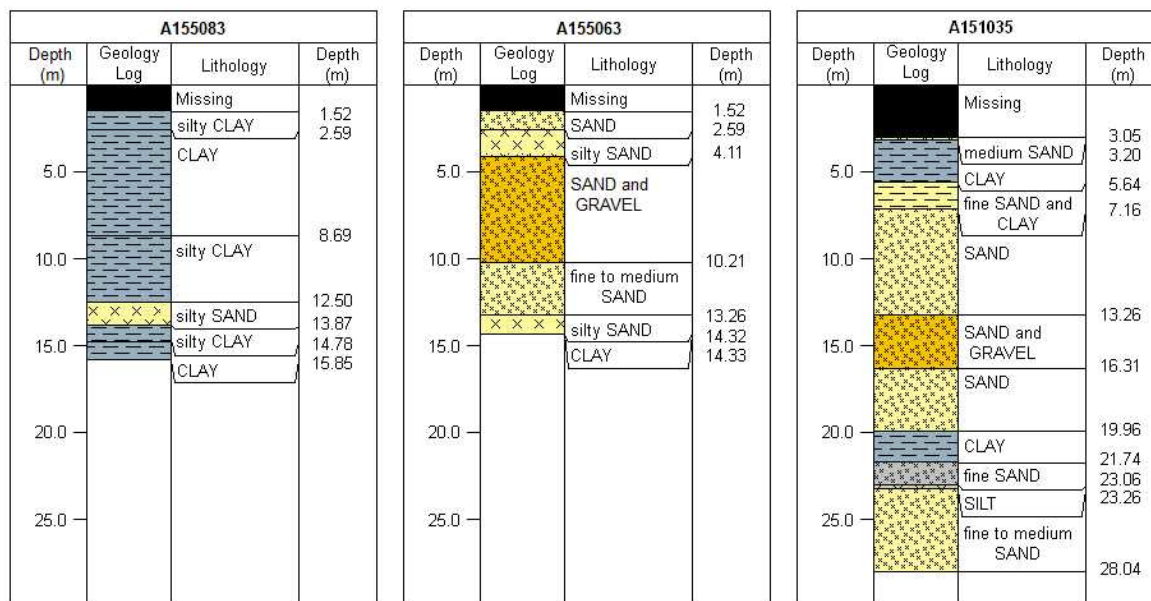
BGS Groundhog® Desktop, Copyright © BGS/UKRI (2021)

Figure 10: Deeper borehole logs (NERC, 2017).

210   **Table 3: Deeper borehole logs and monitoring well details.**

Site / weather station	Trussler Road Farm / WS1	Huron Road Farm / WS3	Bethel Road Farm / WS6
Provincial well tag #	A151035	A155063‡	A155083¶
Easting (m)*	538896.06	536584.58	534185.28
Northing (m)*	4803972.07	4802004.55	4800526.67
Ground surface elevation (m asl)*	371.02	321.88	339.88
Top of casing elevation (m asl)*	372.15	323.13	340.72
Drilling start date	06 Feb 14	12 Feb 14	14 Feb 14
Drilling completion date	10 Feb 14	13 Feb 14	18 Feb 14
Depth of borehole (m bgs†)	28.04	14.33	15.85
Screened interval (m bgs†)	18.29−19.81	0.76−0.87, 2.74−2.85, 4.75−4.86, 6.71−6.82, 8.69−8.80, 10.64−10.75, 12.73−12.84	7.62−9.14
Soil sampling		Split spoon (length: 0.61 m), one sample approximately every 1.5 m	
Type of well	0.051 m diameter PVC	7−port Solinst CMT	0.051 m diameter PVC
Backfill materials within borehole annulus space around casing	bentonite chips (17.7−0.6 m bgs), then cement up to surface	Sand (water table − 1.5 m bgs), then bentonite chips up to ground surface	Sand (9.14−7.62 m bgs), then bentonite chips up to ground surface

* Datum: NAD83, Zone 17N; "m asl" indicates "metres above sea level"

† "bgs" indicates "below ground surface"

‡ Similar installation for well A155050, except that: the well top of casing coordinates were (536540.35 m E,4802045.6 m N, 323.24 m asl); the ground surface elevation was 322.48 m asl; the borehole depth was 15.02 m bgs; and the screened
215   intervals were 2.80−2.91 m bgs, 4.75−4.86 m bgs, 6.66−6.77 m bgs, 8.75−8.86 m bgs, 10.72−10.83 m bgs, 12. 69−12.80 m bgs, and 14.65−14.76 m bgs.

¶ Similar installation for well A155084, except that: the well coordinates were (534185.94 m E, 4800529.31 m N, 340.84 m asl); the ground surface elevation was 340.09 m asl; the borehole depth was 4.57 m; the screened interval was 3.05 m bgs to 4.57 m bgs; sand was backfilled from 4.57 m bgs to 3.05 m bgs, and bentonite was backfilled from 3.05 m bgs up to ground
220   surface.
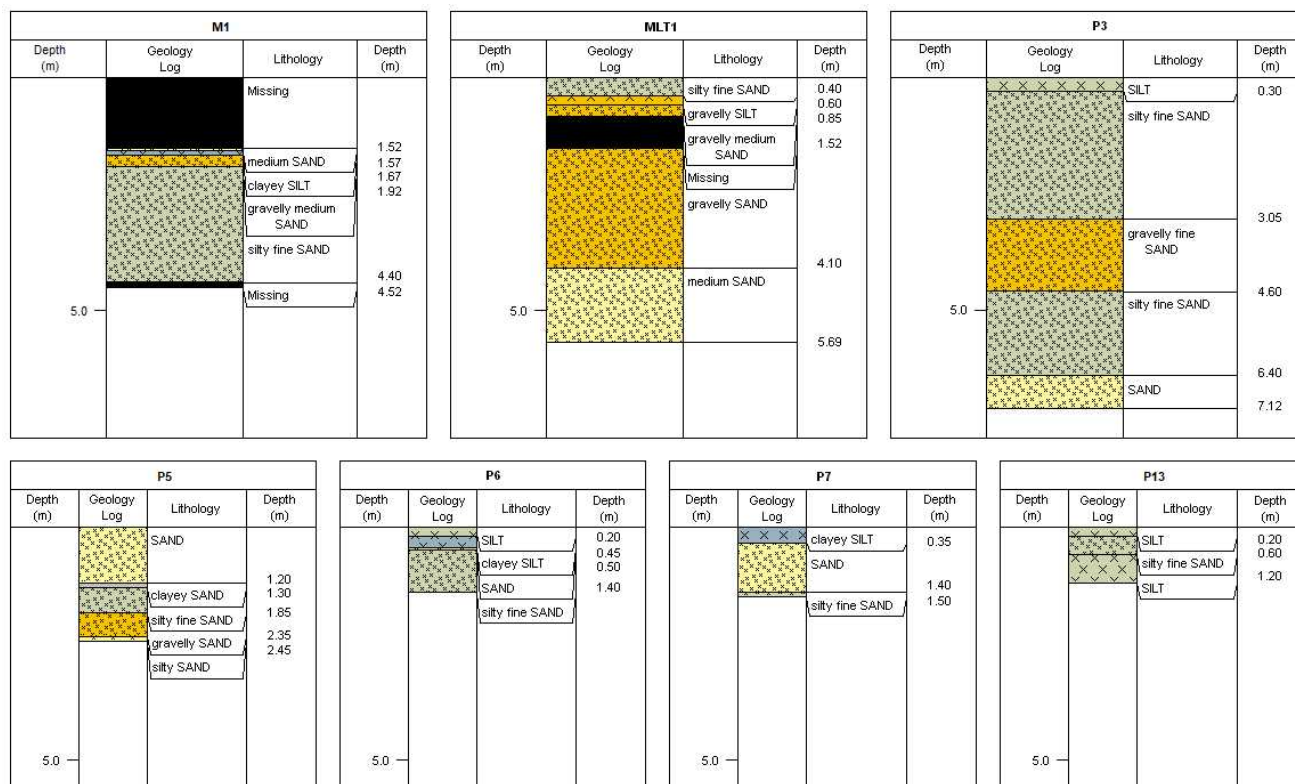
BGS Groundhog® Desktop, Copyright © BGS/UKRI (2021)

Figure 11: Shallow borehole logs (NERC, 2017).

225

Table 4: Bethel Road Farm shallow piezometers (P1 to P13) and borehole logs.

Name	Bottom Depth (m bgs)	Screen Length (m)	Extension of casing above ground surface (m)	Diameter (m)	Installation Date	Comments
P1	4.61	0.3	0.263	0.0254	08 Dec 15	Under active agricultural field
P2	5.60	0.3	0.8	0.0254	08 Dec 15	Under active agricultural field
P3	7.92	0.3	0.87	0.0254	08 Dec 15	Woodlot recharge plot; borehole log collected from core 1 m away
P4	7.01	0.3	0.97	0.0254	08 Dec 15	Woodlot recharge plot
P5	2.67	0.3	0.7	0.0254	08 Dec 15	
P6	1.43	0.3	0.43	0.0254	09 Dec 15	
P7	1.32	0.3	0.54	0.0254	08 Dec 15	
P8	12.77	0.3	0.954	0.0254	09 Dec 15	Screened in medium sand
P9	7.42	0.3	0.45	0.0254	09 Dec 15	
P10	4.46	0.3	0.41	0.0254	09 Dec 15	
P11	5.10	0.3	1.28	0.0254	09 Dec 15	
P12	3.23	0.3	0.43	0.0254	09 Dec 15	
P13	1.09	0.3	0.7	0.0254	16 Dec 15	
M1[*]	4.52	-	-	-	08 Dec 15	Borehole log; water table encountered around 1.3 m bgs[†]
MLT1	5.69	-	-	-	16 Dec 15	Borehole log; water table encountered around 4.1 m; multi−level tensiometer device installed – see Appendix C in Wiebe (2020)

[*] Approximate coordinates: (533820 m E, 4800830 m N, 343 m asl). Coordinates for the other instruments are listed in the Wiebe et al. (2019) dataset.

230   [†] "bgs" indicates "below ground surface"
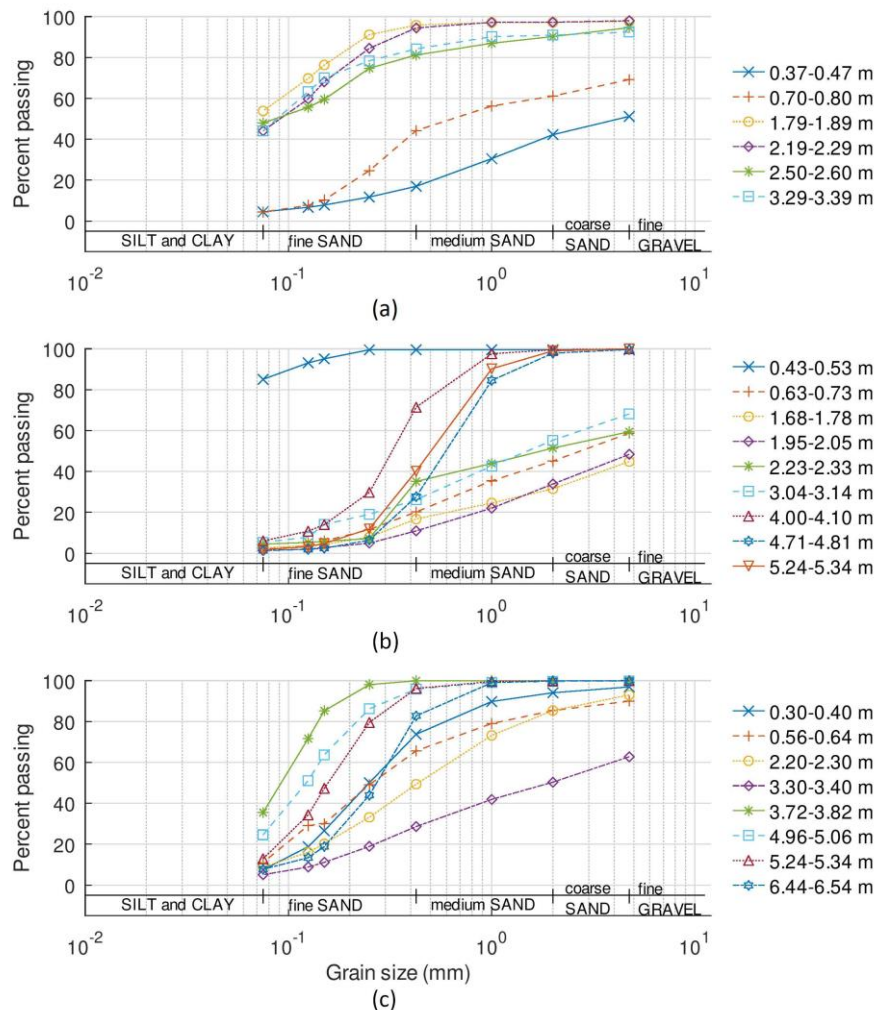
Figure 12: Grain size analyses at (a) Mannheim MLT1, (b) Bethel Road Farm MLT1, and (c) the soil core within 1 m of Bethel
235 **Road Farm P3. Soil sample depth intervals are listed in metres below ground surface. The ground surface elevations for these**
locations are approximately 336.15 m asl, 350.61 m asl, and 349.70 m asl, respectively.

5.2 Soil moisture

Soil moisture was monitored via two sets of eight instruments at the Mannheim site, and one set of eight instruments at the
240 Bethel Road Farm site. Time domain reflectometry (TDR; 0.3 cm sensor length; TDR100, Campbell Scientific Inc.) sensors
and water content reflectometer (0.12 m sensor length; CS655, Campbell Scientific Inc.) instruments were installed at depths
between 0 m and 1.5 m at the Mannheim site, and the water content reflectometer sensors were also installed at depths
between 0 and 1.11 m at the Bethel Road Farm site (Table 5).

Table 5: Soil moisture sensors.

Site	Sensor name	Angle from vertical (°)	Total distance along angle to end of probe (m)	Vertical depth of top of sensor (m)	Vertical depth of bottom of sensor (m)
Mannheim	TDR1	0	-	0.00	0.30
	TDR2	0	-	0.31	0.61
	TDR3	0	-	0.00	0.30
	TDR4	0	-	0.30	0.60
	TDR5	0	-	1.20	1.50
	TDR6	0	-	0.00	0.30
	TDR7	0	-	0.30	0.60
	TDR8	0	-	0.61	0.91
Mannheim	CS655-1'	45	0.5	0.27	0.35
	CS655-2'	45	0.69	0.40	0.49
	CS655-3'	45	0.44	0.23	0.31
	CS655-4'	45	0.89	0.54	0.63
	CS655-5'	0	-	0.00	0.12
	CS655-6'	0	-	0.15	0.27
	CS655-7'	0	-	0.38	0.50
	CS655-8'	0	-	0.19	0.31
Bethel Road Farm	CS655-1	45	0.68	0.40	0.48
	CS655-2	45	1.11	0.70	0.78
	CS655-3	45	1.52	0.99	1.07
	CS655-4	0	-	0.37	0.49
	CS655-5	0	-	0.66	0.78
	CS655-6	0	-	0.99	1.11
	CS655-7	0	-	0.69	0.81
	CS655-8	0	-	0.84	0.96

245

5.3 Soil temperature

Vadose zone temperature profiles were monitored via three approaches. In the first approach, six or seven Tidbit v2 (Onset Computer Corp.) temperature sensors were fixed onto each of three 2.54 cm diameter solid stem PVC rods at intervals and

250   then the rods were installed into separate boreholes drilled using a 7720DT GeoProbe® drill rig with a direct–push system. The three boreholes were installed in locations where different conditions were expected at the Mannheim site (e.g., beneath anticipated ponding in the base of the topographic depression, and at background locations with higher elevations). The sensors on each rod recorded temperatures at depths between 0.1 m and 1.6 m. The boreholes were about the same size as the diameter of the PVC pole so that there was minimal annulus space to backfill. Menkveld (2019) used a similar approach

255 and shows examples of how a vertical temperature profile may be contoured over time with these data to produce 2D plots. In the second approach, six CS109 (Campbell Scientific Inc.) probes were mounted on the outside of 12 mm diameter PVC rods and installed at different depths in individual boreholes. Boreholes were either hand augered or drilled with the drill rig, and then soil was backfilled around the rods, tamping periodically. This later approach was applied in the base of a topographic depression (Mannheim site) that experienced periodic ponding; the temperature sensors were installed at

260 different depths in the vadose zone and used to assess infiltration. Figure 13 shows soil temperature fluctuations over nearly 3 annual cycles. As a third approach, the water content reflectometer sensors also included temperature monitoring capability at the one recharge plot at the Mannheim site and at the Woodlot plot at the Bethel Road Farm site (Fig. 3; Wiebe, 2020).
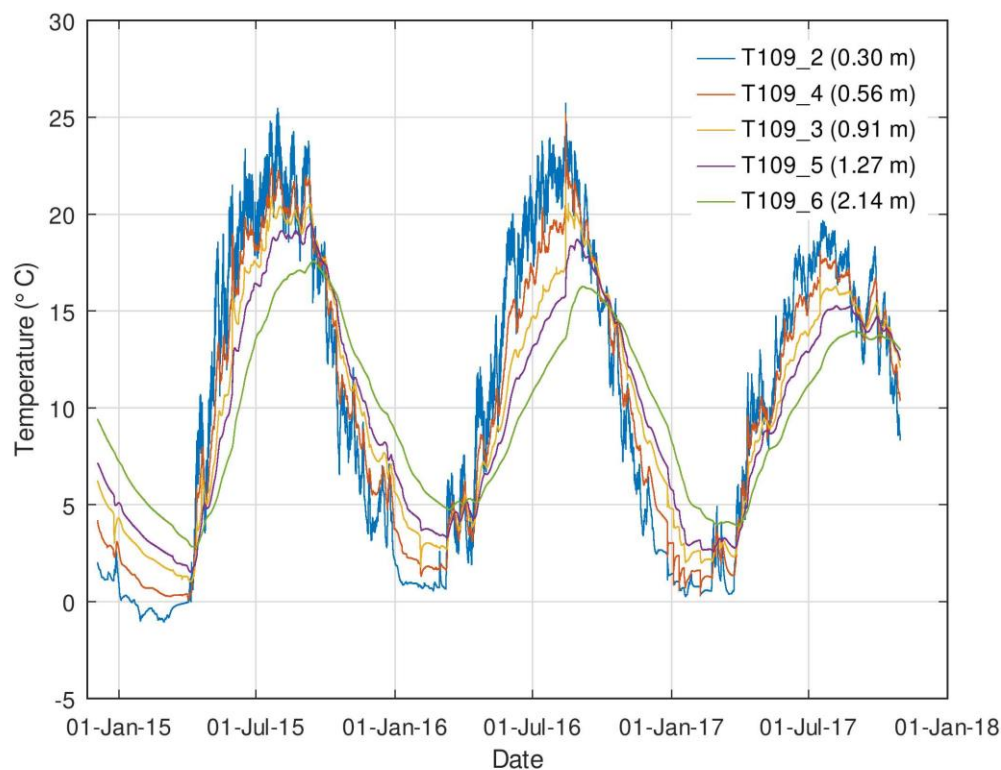
265 **Figure 13: Average daily soil temperatures (Wiebe et al., 2019) at five depths beneath the base of a topographic depression at the Mannheim site.**

The method of Stallman (1965) was used to estimate annual DFR (as vadose zone drainage) at the Mannheim site using data from the CS109 soil temperature sensors (Fig. 12). The idea for this analysis is mentioned by Nimmo et al. (2005)

270 in connection with surface water but was applied here solely to soil temperatures monitored in the base of the topographic depression. The Stallman (1965) method assumes steady state flow and employs the following equations:

$$T(t, z) = T_0 + (\Delta T)\exp(-az)\sin(2\pi t/\tau - bz) , \tag{1}$$

$$K' = \frac{\pi C_b}{\kappa_b \tau} , \tag{2}$$

$$V' = \frac{q C_w}{2\kappa_b} , \tag{3}$$

275

$$a = \left[\left(K'^2 + V'^4/4\right)^{1/2} + V'^2/2\right]^{1/2} - V' , \tag{4}$$

$$b = \left[\left(K'^2 + V'^4/4\right)^{1/2} + V'^2/2\right]^{1/2} , \tag{5}$$

where T is temperature as a function of time (t) and depth (z), T_0 is the mean temperature in surface water (i.e., soil temperature sensor at 0.3 m depth, here), ΔT is the amplitude of temperature fluctuation in surface water (i.e., soil temperature sensor at 0.3 m depth, here; either $|\max(T) - T_0|$ or $|\min(T) - T_0|$), τ is the period of fluctuation (e.g., one year),

280 C_b is the volumetric bulk heat capacity of the soil, κ_b is the bulk aquifer thermal conductivity, q is the vadose zone drainage flux, and C_w is the volumetric heat capacity of water. The lower limit that the method can resolve is about 1×10^{-8} m·s^{-1} or about 1 mm·d^{-1} (Stallman, 1965). The parameters C_b and κ_b were obtained from Brookfield (2009), and C_w was obtained from Palmer et al. (1992). PEST (Doherty, 2015) was used to calibrate the parameters T_0, ΔT, q, and a time offset factor added to t to optimize the fit. Supplementary Materials Document S1 lists the parameters, input files, and GNU Octave

285 (Eaton et al., 2019) scripts used for parameter estimation via PEST; input files for this process were created by calculating daily averages from the 15 min temperature data and then configuring the necessary input file formats required by PEST. Temperature observations from five of the six sensors (T109_2 to T109_6) were used, with equal weighting selected for simplicity. The uppermost sensor (T109_1) was not used because of its wide range of fluctuations, likely influenced by solar radiation heating the shallow soil. Figure 14 shows the results of matching the soil temperature data at three of the five

290 sensor depths and suggests an average recharge flux of 3.5×10^{-8} m·s^{-1} (1,100 mm·yr^{-1}). This seems reasonable considering that local observations suggest that DFR events occur about four times per year on average (Wiebe, 2020) and that recharge rates during such events could range up to 400 mm per event (Wiebe et al., 2021).
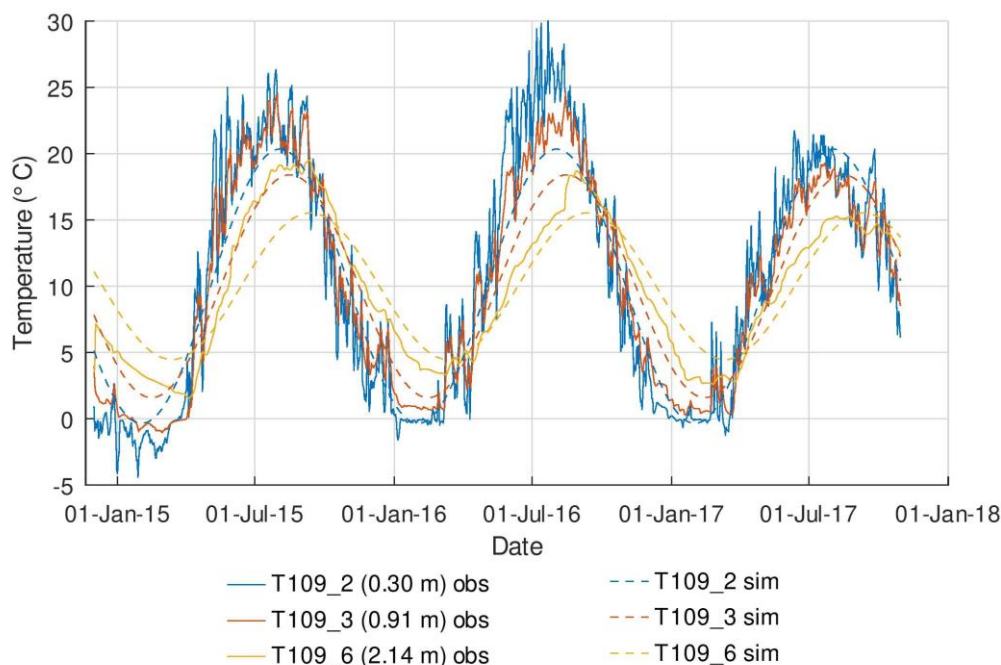
295   **Figure 14: Observed (obs; Wiebe et al., 2019) and simulated (sim) soil temperatures at the Mannheim site for a vadose zone drainage rate of 8.1×10⁻⁸ m·s⁻¹.**

Recharge rates can also be approximated using temperature data at shorter time scales, though the assumption of steady state requires more verification than may be necessary when using longer time scales. The Shan and Bodvarsson

300   (2004) method was applied using the "Flux-LM" spreadsheet tool by Kurylyk et al. (2017) to estimate the vadose zone drainage rate at the Mannheim site for one day in December 2014, as an example of a time when steady state drainage conditions were approximated. The day selected (11 Dec 2014) was more than two weeks after a large infiltration event, and average daily temperatures changed less than 0.1 °C from the previous day at each sensor. The Shan and Bodvarsson (2004) method allows estimation of the average drainage flux (q) through a series of soil layers. The method assumes a 1D vertical

305   soil profile consisting of n layers with values d_i designating their bottom depths. The following equations related to this method are from Shan and Bodvarsson (2004). The steady state governing equation for heat transport through the system is:

$$\alpha_i \frac{d^2 T_i}{dz^2} = q \frac{dT_i}{dz} \qquad (i = 1,2,\ldots,n),$$ (6)

where z is the depth (m), T_i is the temperature (°C) at a point within layer i, and q is the average drainage flux across all layers. The thermal diffusivity (m²·s⁻¹) of the ith layer, α_i, is the ratio:

310    $$\alpha_i = \frac{\lambda_i}{\rho c} \qquad (i = 1,2,\ldots,n),$$ (7)

where λ_i is the thermal conductivity (W·m^{-1}·K^{-1}) of layer i, ρ is the water density (kg·m^{-3}), and c is the heat capacity of water (J·m^{-3}·K^{-1}). Boundary conditions (constant temperature) for the top and bottom of the system, respectively, are:

$$T_1(d_0) = T_0, \tag{8a}$$

$$T_n(d_n) = T_B, \tag{8b}$$

where $d_0 = 0$ m and the conditions at the layer interfaces require that:

$$T_i(d_i) = T_{i+1}(d_i) \qquad (i = 1,2,\dots,n-1). \tag{9}$$

The general solution of Eqn. 6 for temperature variations within layer i is:

$$T_i(z) = C_{i.1}e^{qz/\alpha_i} + C_{i.2} \qquad (i = 1,2,\dots,n), \tag{10}$$

where $C_{i.1}$ and $C_{i.2}$ are integral constants defined by:

$$C_{i.2} = \frac{aT_0 - T_B}{a-1}, \tag{11a}$$

$$C_{1.1} = \frac{T_0 - T_B}{a-1}, \text{ and} \tag{11b}$$

$$C_{(i+1).2} = e^{qd_i(1/\alpha_i - 1/\alpha_{i+1})}C_{i.1} \qquad (i = 1,2,\dots,n-1). \tag{11c}$$

The variable a is defined as:

$$a = e^{qd_n/\alpha_{eff}}, \tag{12}$$

where d_n is the overall thickness and α_{eff} is the effective thermal diffusivity over the n layers:

$$\alpha_{eff} = d_n / \sum_{i=1}^{n}(d_i - d_{i-1})/\alpha_i. \tag{13}$$

Both a one– (thermal) layer model and a two– (thermal) layer model were tested, with slightly better results in terms of root mean square error (0.09 °C vs 0.13 °C) from the two–layer model. Data (Table 6) from the six CS109 sensors were applied with thermal conductivity layer estimates of 1.0 W·m^{-1}·°C^{-1} for the silty uppermost 0.8 m layer of soil, and a value of 2.0 W·m^{-1}·°C^{-1} was applied to the underlying gravelly and sandy materials. These thermal conductivity values were chosen to be generally consistent with the literature for different soil types (e.g., Stonestrom and Constantz, 2003). The flux magnitude was estimated to be 1.2×10^{-7} m·s^{-1} (10 mm·d^{-1}), and the observed and simulated results are shown in Fig. 15.

335 **Table 6: Temperature data (Wiebe et al., 2019) used for Flux-LM (Kurylyk et al., 2017) vadose zone drainage estimate for 12:00 pm on 11 Dec 2014.**

Site	Sensor name	Depth * (m)	Temperature (°C)
	CS109-1	0.08	-0.966
	CS109-2	0.30	1.219
Mannheim	CS109-4 †	0.56	3.154
	CS109-3 †	0.91	5.355
	CS109-5	1.27	6.425
	CS109-6	2.14	8.760

* Depth of bottom of sensor (0.06 m length)

† Please note that the numbering order of the sensors differs slightly from the depth order of the sensors.

340
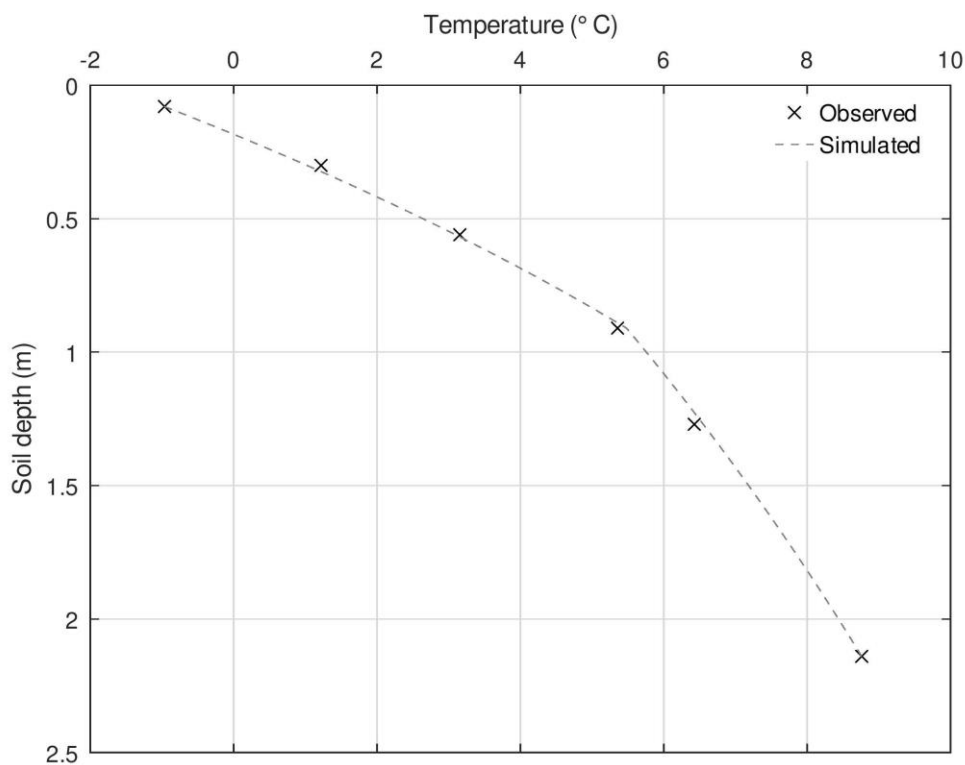
Figure 15: Observed (Wiebe et al., 2019) and simulated soil temperatures at the Mannheim site for 12:00 pm on 11 Dec 2014 for a vadose zone drainage rate of 1.2×10^{-7} m·s⁻¹.

345 **6 Creek data**

Rating curves were compiled from manual stream gauging measurements with a wading rod instrument. The curves mostly captured low and moderate flow conditions and are generally lacking high flow conditions. One high flow condition was roughly estimated for the Huron Road Farm site during an April snowmelt event. Figure 16 shows the rating curves at five sites along the creek. Creek water levels and temperatures were recorded at several of these sites. For example, Fig. 17

350 shows creek water levels at the Huron Road Farm site and streamflow estimated via the rating curve for the site. Either vented (PT12; AquiStar Inc.) or non−vented (Levelogger; Solinst Inc.) pressure transducers were used at the stream stations.
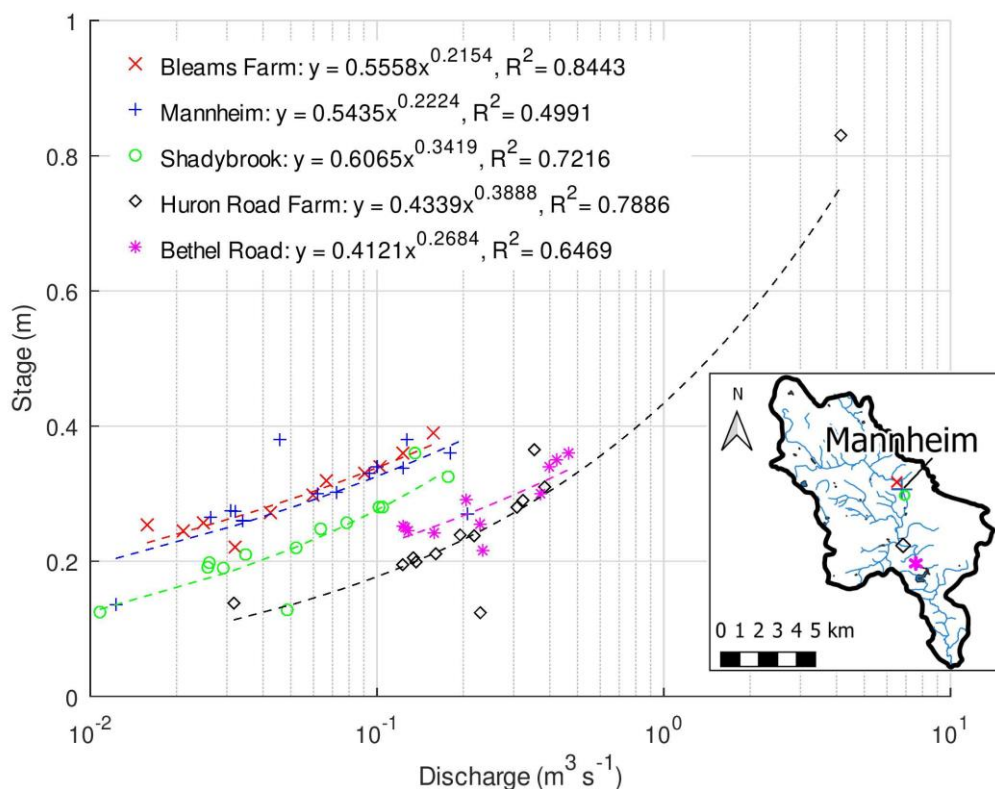
Figure 16: Rating curves (Wiebe et al., 2019) at five locations along the creek (map: DMTI, 2011; GRCA, 1998).

355
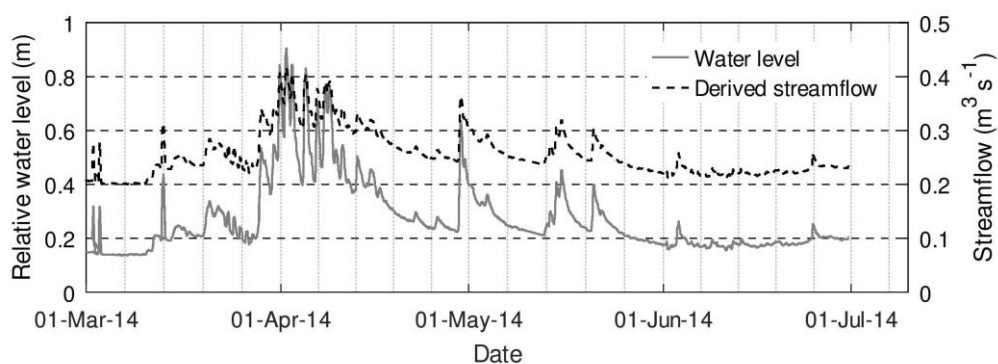
Figure 17: Creek water levels (Wiebe et al., 2019; subsampled at a 1 hour time scale) and streamflow estimates.

7 Geochemistry data

360   Sampling was conducted to record snapshots of the geochemistry of Alder Creek, snowpack within the watershed, and groundwater. Samples were analyzed for major cation and anion concentrations and for O−18 and H−2 isotopes. Nitrate, chloride, sulfate, dissolved oxygen, pH, and turbidity data were collected at several locations within the creek during the summer of 2013. Snow and creek samples were collected and analyzed for O−18 and H−2 isotopes as well as nitrate, chloride, sulfate, soluble reactive phosphorus (SRP), and total phosphorus concentrations during Feb−Apr 2014. Figure 18

365   shows total phosphorus and SRP concentrations in the creek at five sites from Mar−Jun 2014, and Fig. 19 shows isotope data for creek, groundwater, and snow samples.
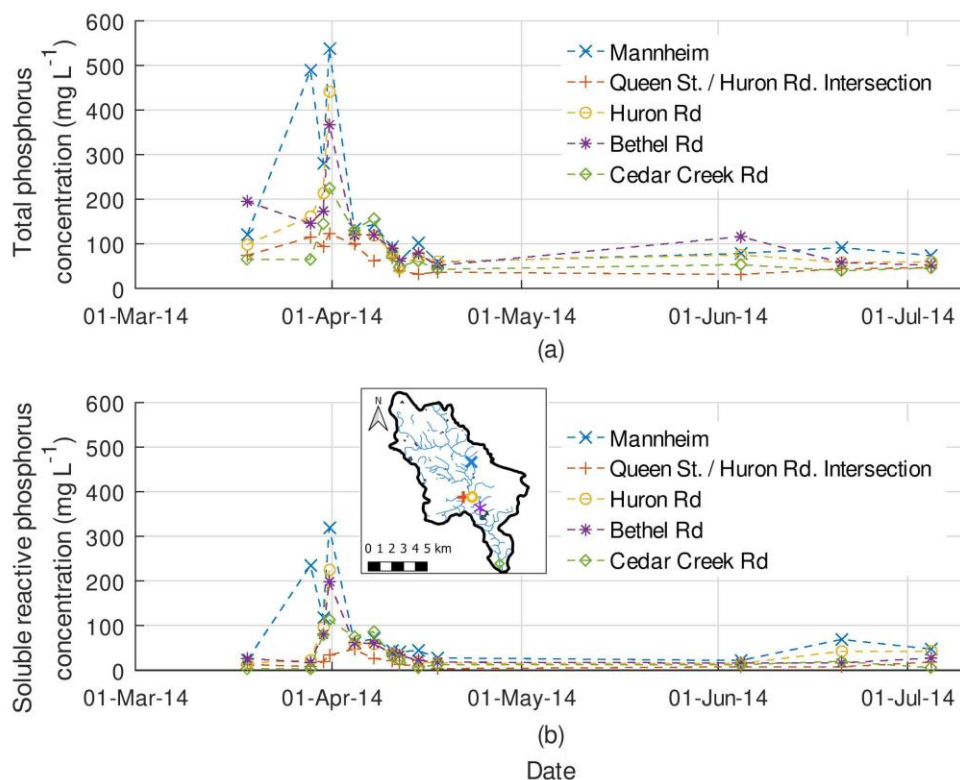
Figure 18: (a) Total phosphorus and (b) SRP concentrations at five sites along the creek in Mar−Jun 2014 (Wiebe et al., 2019;
370 **map: DMTI, 2011; GRCA, 1998). Fig. 17 shows the creek water levels and flow estimates during this time period.**
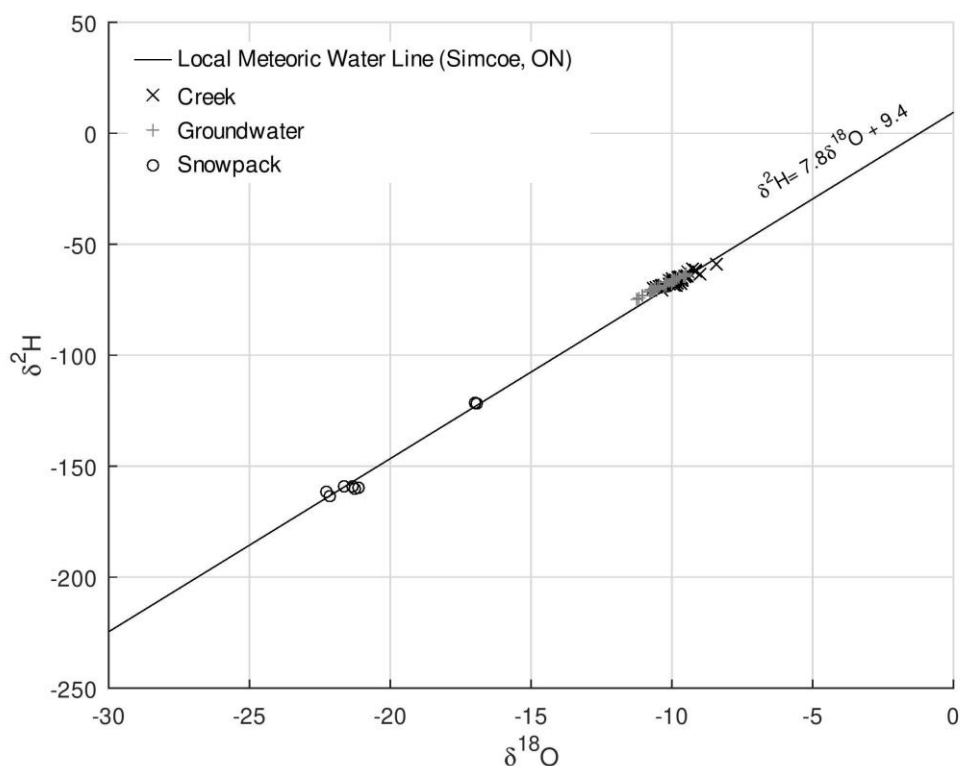
Figure 19: Isotope data from the watershed (Wiebe et al., 2019; local meteoric water line from Bajc et al., 2018).

8 Data availability

375 All data presented in this paper are available from the Federated Research Data Repository (https://doi.org/10.20383/101.0178; Wiebe et al., 2019). Equipment or sampling locations corresponding to where the data were collected are provided in several GIS shapefiles included in the dataset. The files of the dataset may be downloaded without creating a user account by right–clicking the individual files of interest, selecting "Save Link As...", and preserving the file extensions. Table 7 summarizes the time periods associated with the data.

380 Several papers and theses have employed the data presented above: Hillier (2014), Menkveld (2019), Wiebe and Rudolph (2020), Wiebe (2020), and Wiebe et al. (2021).

9 Code availability

Supplementary Materials Document S1 contains background information for the optimization of the parameters for the Stallman (1965) method. The file includes GNU Octave (Eaton et al., 2019) scripts and file formats used to conduct

385 parameter estimation via PEST (Doherty, 2015).

Table 7: Data availability.

Parameter(s)	Site/Location	Time Period
Air temperature and relative humidity	WS1 – WS7	May 2013 – Dec 2018
Wind speed and direction	WS1 – WS7	May 2013 – Dec 2018
Rainfall	WS2 – WS7	May 2013 – Dec 2018
Snowfall	WS2 – WS7	Nov 2014 – Apr 2015
Solar radiation	WS1 – WS7	May 2013 – Dec 2018
Barometric pressure	WS4	May 2015 – Apr 2018
	WS7	Dec 2013 – Apr 2017
Manual water levels	all wells	Jan 2014 – Dec 2018 (occasional)
Pressure transducer water levels and temperatures (observation wells)	Mannheim, Bethel Farm	Nov 2014 – Apr 2018
	Huron Rd. Farm (CMT4)	Mar 2014 – Dec 2018
Soil moisture and electrical conductivity	Mannheim – TDR system	Nov 2014 – Jun 2018
	Mannheim – CS655 system [†]	Dec 2015 – Jun 2018
	Bethel Rd Farm – CS655 [†]	Jun 2016 – Jul 2019
Soil temperature	Mannheim – TidbiT poles	Nov 2017 – Apr 2018
	Mannheim – CS109	Nov 2014 – Jun 2018
Relative barometric pressure [*]	Mannheim	Nov 2015 – Oct 2017
	Bethel Rd Farm	Mar 2016 – May 2018
Creek water levels and temperatures	Mannheim – WL5 North	Jul 2014 – Jun 2017
	Mannheim – transect PT12	Nov 2014 – Apr 2018
	Mannheim – RR1	Nov 2013 – Apr 2018
	Huron Rd. Farm	Aug 2013 – May 2014
	Bethel Rd Bridge	Aug 2013 – Jun 2015
	Cedar Creek Rd Bridge	Sep 2014 – Dec 2016
Anion concentrations (Cl^-, SO_4^{2-}, NO_3^-)	Consistently at 5 locations along creek	4× from Jul – Aug 2013, and 14× from Mar–Jul 2014
Total phosphorus and soluble reactive phosphorus	5 locations along creek	14× from Mar–Jul 2014
$\delta^{18}O$ and δ^2H isotope concentrations in creek, groundwater, and snow	Multiple locations along creek; Mannheim CMT wells; snow at WS1 to WS6	10× from Jul 2013 – Feb 2014
Temperature, electrical conductivity, total suspended solids, total dissolved solids, specific conductivity, salinity, non–linear function electrical conductivity, dissolved oxygen, barometric pH, turbidity	Consistently at 5 locations along creek	14× from Mar–Jul 2014
Anion (Cl^-, NO_2^-, NO_3^-, PO_4^{3-}, SO_4^{2-}) and cation (Na^+, NH_4^+, K^+, Mg^{2+}, Ca^{2+}) concentrations	Snow at WS1, WS3, WS4, WS6; creek samples from various locations	Feb 2014 (snow and creek), Mar 2014 (creek)

[*] For correcting non–vented pressure transducers; Solinst Barologger data for the Mannheim and Bethel Road Farm sites may also be used for corrections

[†] Also includes temperature

390

10 Summary

Hydrological and meteorological instruments were deployed in the Alder Creek watershed between 2013 and 2018. This watershed provides source water to several well fields, and the data have been used within numerical models estimating groundwater recharge. A new analysis of vertical soil temperature profile records presented above suggested that annual
395 drainage rates related to ponding in the base of a topographic depression at the Mannheim site could be around 1,100 mm per year from 2015 to 2017. Despite the short duration of the data collection (3 to 4 years), it is hoped that the data may be useful to other researchers and instructors.

Supplement link

Supplementary Materials Document S1.pdf ("GNU Octave code and PEST file formats employed for vadose zone drainage
400 calculations").

Author Contribution

Conceptualization, AW; methodology, AW; software, AW; formal analysis, AW; investigation, AW; resources, DR; data curation, AW; writing – original draft preparation, AW; writing – review and editing, DR, AW; visualization, AW; supervision, DR; project administration, DR; funding acquisition, DR, AW.

405 ### Competing interests

The authors declare that they have no conflict of interest.

Acknowledgements

We acknowledge the support of the Natural Science and Engineering Research Council of Canada (NSERC; IPS Grant #485430 to A.J. Wiebe, and Discovery Grant to D.L. Rudolph). The Global Water Futures project of the Canada First
410 Research Excellence Fund provided the resources for publishing the dataset online. Field equipment was provided by the Southern Ontario Water Consortium (Ontario MEDI, Project #21616; FedDev Ontario, Project #801680). Thanks to the many students and technicians who assisted with the field work and data collection: P. Johnson, B. Ingleton, O. Idika, S. McKay, J. Dickhout, K. Blowes, L. Harrison, C. Hillier, J. Robertson, J. Elliott, E. Mesec, P. Menkveld, N. Couperus, N. Long, J. Stevens, I. Mercer, E. Pai, E. Huang, S. Indris, J. Ju, J. Leon, and A. Wicke. Thanks to E. Mesec, E. Pai, P.
415 Menkveld, and E. Huang for assisting with borehole logging, to E. Huang for conducting the grain size analyses, and to E. Mesec and L. Harrison for collecting the geochemistry and isotope samples. We are indebted to the individuals, businesses,

and local governments who agreed to host field equipment during the study: R. and W. Goettling, G. and L. Kaster, D. and P. Mighton, the Region of Waterloo, Colour Paradise Greenhouses, Herrle's Farm Market, Nith Valley Organics, Rebel Creek Golf Club, and the County of Oxford.

420 **References**

Bajc, A.F., Marich, A.S., Priebe, E.H., and Rainsford, D.R.B.: Evaluating the groundwater resource potential of the Dundas buried bedrock valley, southwestern Ontario: an integrated geological and hydrogeological case study, Can. J. Earth Sci., 55(7), 659–676, doi:10.1139/cjes-2016-0224, 2018.

Bajc, A.F., Russell, H.A.J., and Sharpe, D.R.: A three-dimensional hydrostratigraphic model of the Waterloo Moraine area,
425 southern Ontario, Canada, Can. Water Resour. J., 39(2), 95–119, doi:10.1080/07011784.2014.914794, 2014.

Brookfield, A.E.: Simulation of thermal energy transport in a fully–integrated surface/subsurface framework, PhD. dissertation, University of Waterloo, Waterloo, ON, Canada, http://hdl.handle.net/10012/4318, 2009.

Brouwers, M.H.: A case study for assessing the hydrologic impacts of climate change at the watershed scale, MASc. thesis, University of Waterloo, Waterloo, ON, Canada, http://hdl.handle.net/10012/3514, 2007.

430 Constantz, J.: Heat as a tracer to determine streambed water exchanges, Water Resour. Res., 44, W00D10, doi:10.1029/2008WR006996, 2008.

CH2MHILL, and S.S. Papadopulos and Associates Inc. (SSPA): Alder Creek Groundwater Study: Final Report, Prepared for: The Regional Municipality of Waterloo, CH2MHILL, Kitchener, ON, Canada, 2003.

DMTI Spatial Inc. (DMTI): CanMap Streetfiles, major water regions, and minor water regions [data set], obtained from
435 University of Waterloo Geospatial Centre, Waterloo, ON, Canada, controlled access, last access: 29 Mar 2012, 2011.

Doherty, J.: Calibration and Uncertainty Analysis for Complex Environmental Models, Watermark Numerical Computing, Brisbane, Australia, ISBN 978-0-9943786-0-6, 2015.

Eaton, J.W., Bateman, D., Hauberg, S., and Wehbring, R.: GNU Octave, A high-level interactive language for numerical computations, Edition 5 for Octave version 5.1.0, https://www.gnu.org/software/octave/, last access: 04 Jul 2019.

440 Esri, HERE, Garmin, Intermap, increment P Corp., GEBCO, USGS, FAO, NPS, NRCAN, GeoBase, IGN, Kadaster NL, Ordnance Survey, Esri Japan, METI, Esri China (Hong Kong), swisstopo, © OpenStreetMap contributors, and the GIS User Community: World topographic map [GIS data set], http://goto.arcgisonline.com/maps/World_Topo_Map, last access: 02 Nov 2020, 2020a.

Esri, HERE, Garmin, © OpenStreetMap contributors, and the GIS user community: Light grey canvas base, World map [GIS
445 data set], http://goto.arcgisonline.com/maps/World_Light_Gray_Base, last access: 02 Nov 2020, 2020b.

Government of Canada: Historical Data: Rainfall, snowfall, and temperature data for the Roseville, ON, weather station [data set], http://climate.weather.gc.ca/historical_data/search_historic_data_e.html, last access: 15 Jan 2019.

Grand River Conservation Authority (GRCA): Subcatchment basins [data set], https://maps.grandriver.ca/data-gis.html, last access: 29 Mar 2012, 1998.

450 Hillier, C.E.: Establishing metrics to quantify the vulnerability of municipal supply wells to contaminants from surface water sources, MSc. thesis, University of Waterloo, Waterloo, ON, Canada, http://hdl.handle.net/10012/8683, 2014.

Irvine, C.A.: Effects of land use and hydrophysical drivers on temporal and spatial variability of phosphorus and nitrate export in an agricultural subwatershed in southern Ontario, Canada, MSc. thesis, University of Waterloo, Waterloo, ON, Canada, http://hdl.handle.net/10012/12885, 2018.

455 Kurylyk, B.L., Irvine, D.J., Carey, S.K., Briggs, M.A., Werkema, D.D., and Bonham, M: Heat as a groundwater tracer in shallow and deep heterogeneous media: Analytical solution, spreadsheet tool, and field applications, Hydrol. Process., 31, 2648–2661, doi:10.1002/hyp.11216, 2017.

Lerner, D.N., Issar, A.S., and Simmers, I.: Groundwater recharge. A guide to understanding and estimating natural recharge, International contributions to hydrogeology, Volume 8, International Association of Hydrogeologists, Heise, Hannover,
460 Germany, https://iah.org/education/professionals/out-of-print-books, 1990.

Martin, P.J., and Frind, E.O.: Modeling a complex multi–aquifer system: The Waterloo Moraine, Ground Water, 36(4), 679–690, doi:10.1111/j.1745-6584.1998.tb02843.x, 1998.

Matrix Solutions Inc. (Matrix), and S.S. Papadopulos and Associates Inc. (SSPA): Region of Waterloo Tier Three Water Budget and Local Area Risk Assessment, Final Report, Sep 2014, Prepared for: Region of Waterloo, Matrix Solutions Inc.,
465 Kitchener, ON, Canada, https://www.sourcewater.ca/en/source-protection-areas/resources/Documents/Grand/RMOW-September-2014-WQRA_chpt-1-10.pdf, 2014.

Menkveld, P.G.: A field study of event based, seasonally affected, depression focused recharge in glaciated terrain, MSc. thesis, University of Waterloo, Waterloo, ON, Canada, http://hdl.handle.net/10012/14568, 2019.

Natural Environment Research Council (NERC): BGS Groundhog® Desktop Geoscientific Information System, Version
470 1.10.0, British Geological Survey, UK [software], https://www.bgs.ac.uk/technologies/software/groundhog/, last access: 02 May 2019, contains public sector information licensed under the Open Government Licence v3.0, https://www.nationalarchives.gov.uk/doc/open-government-licence/version/3/, 2017.

Nimmo, J.R., Healy, R.W., and Stonestrom, D.A.: Aquifer Recharge, in: Encyclopedia of Hydrological Science: Part 13, Groundwater, edited by: Anderson, M.G., and Bear, J., Wiley, Chichester, UK, v.4, 2229–2246,
475 doi:10.1002/0470848944.hsa161a, 2005.

Ontario Geological Survey (OGS): Surficial geology of southern Ontario, Miscellaneous Release--Data 128-REV [data set], ISBN 978-1-4435-2482-7, obtained from Matrix Solutions Inc., Guelph, ON, Canada, controlled access, last access: 29 Jun 2016, 2010.

Ontario Ministry of Natural Resources (OMNR): Southern Ontario Land Resource Information System (SOLRIS) Land Use
480 Data [data set], obtained from University of Waterloo Geospatial Centre, Waterloo, ON, Canada, controlled access, last access: 03 Jun 2009, 2008.

Ontario Ministry of Natural Resources and Forestry (OMNRF): Enhanced watercourse, Ontario Integrated Hydrology Data [data set], updated 05 Oct 2015, https://geohub.lio.gov.on.ca/, last access: 02 May 2018, 2015.

Palmer, C.D., Blowes, D.W., Frind, E.O., and Molson, J.W.: Thermal energy storage in an unconfined aquifer: 1. Field
485 injection experiment, Water Resour. Res., 28(10), 2845−2856, doi:10.1029/92WR01471, 1992.

Province of Ontario: Map, Well records, www.ontario.ca/page/map-well-records, last access: 4 Nov 2021, 2021.

Region of Waterloo (ROW): Land use data for Kitchener (31 Aug 2010), Waterloo (24 Sep 2009), and Wilmot (24 Sep 2009) [data set], obtained from Matrix Solutions Inc., Guelph, ON, Canada, controlled access, last access: 21 Jun 2016, 2010.

490 Raes, D.: The ETo Calculator: Evapotranspiration from a reference surface, Reference Manual Version 3.1, Food and Agriculture Organization of the United Nations, Land and Water Division, Rome, IT, http://www.fao.org/land-water/databases-and-software/eto-calculator/en/, last access: 01 Feb 2018, 2009.

Seglenieks, F.: University of Waterloo Weather Station Data Archives [data set], http://weather.uwaterloo.ca/data.html, last access: 09 Oct 2020.

495 Shan, C., and Bodvarsson, G.: An analytical solution for estimating percolation rate by fitting temperature profiles in the vadose zone, J. Contam. Hydrol., 68, 83−95, doi:10.1016/S0169-7722(03)00126-8, 2004.

Solinst Canada, Ltd. (Solinst): Solinst Technical Bulletin: Barometric Compensation and the Importance of Barometric Data, Solinst Canada Ltd., Georgetown, ON, Canada, https://www.solinst.com/onthelevel-news/water-level-monitoring/water-level-datalogging/barometric-compensation-and-the-importance-of-barometric-data/, last access: 4 Nov 2021, 2020.

500 Sousa, M.R., Jones, J.P., Frind, E.O., and Rudolph, D.L.: A simple method to assess unsaturated zone time lag in the travel time from ground surface to receptor, J. Contam. Hydrol., 144(1), 138−151, doi:10.1016/j.jconhyd.2012.10.007, 2013.

Stallman, R.W.: Steady one−dimensional fluid flow in a semi−infinite porous medium with sinusoidal surface temperature, J. Geophys. Res., 70(12), 2821−2827, doi:10.1029/JZ070i012p02821, 1965.

Stonestrom, D.A., and Constantz, J.: Heat as a tool for studying the movement of ground water near streams, United States
505 Geological Survey (USGS) Circular 1260, USGS, Reston, VA, USA, https://pubs.usgs.gov/circ/2003/circ1260, 2003.

Toronto Region Conservation Authority (TRCA): GIS map of the TRCA watersheds [data set], contains information made available under the Toronto and Region Conservation Authority (TRCA)'s Open Data Licence v 1.0, Updated 2 Sep 2020, TRCA, Toronto, ON, Canada, https://data.trca.ca/, last access: 01 Mar 2021, 2018.

Water Survey of Canada (WSC): Daily discharge data for Alder Creek near New Dundee (02GA030)[ON] [data set],
510 https://wateroffice.ec.gc.ca/mainmenu/historical_data_index_e.html, last access: 12 Mar 2019, 2019.

Wiebe, A.J.: The influences of spatially variable rainfall and localized infiltration on groundwater recharge in a water management context, PhD. dissertation, University of Waterloo, Waterloo, ON, Canada, http://hdl.handle.net/10012/16476, 2020.

Wiebe, A.J., Menkveld, P.G., Hillier, C.E., Mesec, E., and Rudolph, D.L.: Meteorological and hydrological data from the
515   Alder Creek watershed, Grand River basin, Ontario [data set], New Digital Research Infrastructure Organization, Toronto,
ON, Canada, doi:10.20383/101.0178, 2019.

Wiebe, A.J., and Rudolph, D.L.: On the sensitivity of modelled groundwater recharge estimates to rain gauge network scale,
J. Hydrol., 585, 124741, doi:10.1016/j.jhydrol.2020.124741, 2020.

Wiebe, A.J., Rudolph, D.L., Pasha, E., Brook, J.M., Christie, M., and Menkveld, P.G.: Impacts of Event−Based Recharge on
520   the Vulnerability of Public Supply Wells, Sustainability−Basel, 13(14), 7695, doi:10.3390/su13147695, 2021.